Finite-temperature dynamics of the spin-$\frac{1}{2}$ bond alternating Heisenberg antiferromagnetic chain

H. J. Mikeska and C. Luckmann
Institut für Theoretische Physik, Universität Hannover, 30167 Hannover, Germany
(Received 21 February 2006; published 19 May 2006)

We present results for the dynamic structure factor of the $S=1/2$ bond alternating Heisenberg chain over a large range of frequencies and temperatures. Data are obtained from a numerical evaluation of thermal averages based on the calculation of all eigenvalues and eigenfunctions for chains of up to 20 spins. Interpretation is guided by the exact temperature dependence in the noninteracting dimer limit which remains qualitatively valid up to an interdimer exchange $\lambda \approx 0.5$. The temperature induced central peak around zero frequency is clearly identified and aspects of the crossover to spin diffusion in its variation from low to high temperatures are discussed. The one-magnon peak acquires an asymmetric shape with increasing temperature. The two-magnon peak is dominated by the $S=1$ bound state which remains well defined up to temperatures of the order of J. The variation with temperature and wave vector of the integrated intensity for one-magnon and two-magnon scattering and of the central peak are discussed.

DOI: 10.1103/PhysRevB.73.184426 PACS number(s): 75.10.Jm, 75.10.Pq, 75.40.Gb, 78.70.Nx

I. INTRODUCTION

Low-dimensional gapped quantum antiferromagnets have received much interest in recent years both experimentally and theoretically. They serve as model substances allowing one to investigate in detail the effects of quantum fluctuations and to test theoretical models. A particularly simple class of materials in this context consists of an assembly of dimers (two strongly coupled spins 1/2) which interact sufficiently weakly to guarantee that the dimer gap does not close. These materials are characterized by a disordered singlet ground state and a finite spin gap to triplet excited states. Materials of this type occur in nature as quasione-dimensional (1D) $[Cu(NO_3)_2 \cdot 2.5H_2O]$,[1] quasitwo-dimensional $(BaCuSi_2O_6)$,[2] and three-dimensional (3D) ($KCuCl_3$ and $TlCuCl_3$) (Refs. 3 and 4) compounds.

Systems of this type are characterized by both quantum and thermal fluctuations: Thermal fluctuations are controlled by the temperature T and the quantum fluctuations of interest in dimer systems (i.e., those modifying the basic quantum mechanics of isolated dimers) are governed by the interdimer coupling. So far, most investigations have concentrated on the quantum aspects, excluding thermal fluctuations by working at zero (theoretically), respectively, low (experimentally) temperature. The theoretical approach is then restricted to the low-lying eigenstates of the quantum Hamiltonian, which are accessible to an approximate analytical treatment or to numerical calculations. However, at finite temperature of the order of or even large compared to the magnetic exchange energy, all levels participate and more elaborate approximations, respectively, numerical approaches are necessary.

Recently increasing interest has developped in the finite temperature behavior of such systems and experimental results for $Cu(NO_3)_2 \cdot 2.5H_2O$ (Refs. 1 and 5) and $TlCuCl_3$ (Ref. 6) demonstrate that an understanding of the interplay of thermal and quantum fluctuations requires additional work on the theoretical and numerical side. Our aim here is to investigate for the system of weakly coupled dimers described above the dynamical structure factor over a wide range of frequencies and temperatures.

To explore from numerical calculations the content of a given Hamiltonian for finite temperatures is more involved than for $T=0$ since the Lanczos approach which allows one to treat reasonably large systems (up to 36 spins $S=1/2$) does not give more than a few low-lying energy levels. Instead, the direct approach to dynamic properties at finite temperatures requires full exact diagonalization (FED) to obtain energies and wave functions; this has been done so far for the XXZ $S=1/2$ chain[7] and the frustrated $S=1/2$ Heisenberg chain[8] up to 16 spins. If FED is restricted to energy levels only, thermodynamic properties such as the specific heat, susceptibility and structure factor $S(q)$ are obtained; this has been done for a number of dimer type systems such as the dimerized and frustrated $S=1/2$ chain[9] and the two-leg ladder.[10] These numerical approaches to finite temperatures have been supplemented by approximate analytical approaches such as including thermal occupation factors in the mean field approach[6,11] and a strong coupling field theoretic approach.[12]

We describe the 1D $S=1/2$ chain with alternating isotropic antiferromagnetic nearest-neighbor exchange [the bond alternating Heisenberg chain (BAHC)] as a system of $N/2$ unit cells with two spins each and two exchange constants, the intradimer exchange J and the interdimer exchange λJ, using the following Hamiltonian:

$$\mathcal{H} = J \sum_{n=1}^{N/2} (\mathbf{S}_{n,1} \cdot \mathbf{S}_{n,2} + \lambda \mathbf{S}_{n,2} \cdot \mathbf{S}_{n+1,1}). \quad (1)$$

We assume $J>0$ and apply periodic boundary conditions. For $\lambda=0$ the ground state of the system consists of singlets on the intradimer bonds $(n,1)-(n,2)$. These local singlets can be excited to triplets which develop into a band of gapped excitations when switching on λ. At higher energies multiparticle excitations dominate the spectrum. In the limit $\lambda=1$ we arrive at the well known Heisenberg antiferromagnetic chain (HAF) with pairs of $S=1/2$ spinons as lowest gapless excitations. Other related models are described in Ref. 13.

The dynamics of such a system is most appropriately discussed in terms of the dynamic structure factor, i.e., the Fourier transform of the time dependent spin correlation function which, apart from well known prefactors gives the spectral weight measured as the magnetic inelastic neutron scattering (INS) cross section.[14] The dynamic structure factor of the BAHC at low temperatures ($T \ll J$) is characterized by a peak due to singlet-triplet transitions as most prominent feature and continua of multiparticle excitations at higher energies. From extended work on the $T=0$ quantum mechanics of this system (Refs. 15–19, and references therein) it is known that finite interdimer coupling λ leads to considerable modifications in energies and transition strengths for one and two magnon processes as well as to the emergence of bound states below (and above) the two magnon band. Here we present results from FED for up to 20 spins for the longitudinal dynamic structure factor (DSF) $S^{zz}(\mathbf{q},\omega)$ for a wide range of temperatures, varying from $T \ll J$ to $T \gg J$. Our discussion will concentrate on the variations of the one and two magnon line shapes with temperature (with particular emphasis on the bound state) and on the temperature dependence of the contributions from the temperature induced, "central peak" at $\omega \approx 0$ which is due to intraband transitions. This peak is the signature of spin diffusion in the classical limit; its temperature dependence has not been discussed so far in a microscopic context, but it is clearly seen in recent INS experiments.[5]

For N spins localized on sites $\mathbf{x}_i$ on a 1D lattice the dynamical structure factor is defined as

$$S^{\alpha\beta}(\mathbf{q},\omega) = \frac{1}{2\pi N}\sum_{i,j}\int_{-\infty}^{\infty} dt e^{i[\mathbf{q}(\mathbf{x}_i-\mathbf{x}_j)-\omega t]} \langle S_i^{\alpha}(t) S_j^{\beta}(t=0)\rangle. \tag{2}$$

The superscripts α,β denote the spin components and the brackets $\langle\cdots\rangle$ thermal expectation values (which for $T=0$ reduce to ground state expectation values $\langle 0|\cdots|0\rangle$). For the isotropic Hamiltonian (no magnetic field) of Eq. (1) the dynamic structure factor is diagonal with three equal components. It is therefore sufficient to restrict the discussion in the following to one component, $S^{zz}(\mathbf{q},\omega)$. In the presence of a magnetic field, a case to be treated in subsequent work, we will have to distinguish between $S^{zz}(\mathbf{q},\omega)$ and $S^{+-}(\mathbf{q},\omega)$.

The remainder of this article is organized as follows: In Sec. II we review and discuss simple limiting situations and our numerical approach, in Sec. III we present results for the BAHC with λ up to 0.3 and temperatures up to $4J$ and in the final Sec. IV we discuss the range of validity of our approach and give our conclusions.

II. LIMITING CASES AND NUMERICAL APPROACH

The BAHC has lattice sites $\mathbf{x}_i = n\mathbf{b} + p\mathbf{d}/2$, $n = 1\cdots N/2$, $p = \pm 1$. Here $\mathbf{d}$ is the intradimer distance, the direction of $\mathbf{d}$ in general differs from the chain direction given by $\mathbf{b}$. At finite temperatures the general expression for $S^{zz}(\mathbf{q},\omega)$ is written as

$$S^{zz}(\mathbf{q},\omega) = \sum_i \frac{e^{-\beta E_i}}{Z}\cdot\sum_k |\langle\psi_k|S^z_{\mathbf{q}}|\psi_i\rangle|^2 \delta[\omega-(\omega_k-\omega_i)], \tag{3}$$

where Z is the partition function and we have introduced the Fourier transformed spin operators

$$S^z_{\mathbf{q}} = \frac{1}{\sqrt{N}}\sum_{n=0}^{N/2-1}\sum_{p=\pm 1} e^{i\mathbf{q}(n\mathbf{b}+p\mathbf{d}/2)} S^z_{n,p}. \tag{4}$$

We begin by reviewing results for the two limiting cases $T=0$ (pure quantum effects) and $\lambda=0$ (pure thermal fluctuations). The BAHC at $T=0$ with its singlet-triplet gap is one of the simplest systems to study strong quantum fluctuations in numerical and analytical approaches. This has been done by many different methods, among them the random phase approximation[15] and series expansions in the coupling strength λ.[16–19] The application of these methods has concentrated on two types of low-lying excitations, i.e., eigenstates of the Hamiltonian, above the singlet ground state: (i) The basic quantum excitation is the first excited triplet, i.e., the propagating one magnon excitation (one excited dimer) and (ii) two magnon excitations which form a continuum with the possibility of bound states. These states are decorated by admixtures of multimagnon excitations which become more and more important when the interdimer coupling λ increases. These methods have established the existence of bound states of two excited dimers below the two magnon band, two singlets and two triplets,[17] for wave vectors close to π and energies and transition matrix elements for the one and two magnon bands have been obtained up to 13th order[18] from series expansions. We remark that the analogous calculation including 3D interactions has only been done up to third order.[19] These results are in excellent agreement with experiments at low temperatures.

In the limit of vanishing coupling, $\lambda=0$, on the other hand, the BAHC reduces to an assembly of noninteracting dimers and its exact dynamical structure factor can be easily calculated for all temperatures. In spite of the simplicity of the calculation the result is instructive as a guide to the general case. The full result for $S^{zz}(\mathbf{q},\omega)$ in this limit is

$$S^{zz}_{\lambda=0}(\mathbf{q},\omega) = \frac{1}{4}\frac{1}{1+3e^{-\beta J}}\{2(1+\cos\mathbf{q}\cdot\mathbf{d})e^{-\beta J}\delta(\omega) + (1-\cos\mathbf{q}\cdot\mathbf{d})[\delta(\omega-J)+e^{-\beta J}\delta(\omega+J)]\}. \tag{5}$$

This expression is valid for any number of spins N. The wave vector $\mathbf{q}$ is in chain direction and q takes only the $N/2$ discrete values $q=(2\pi m)/(Nb/2)$, $m=1,2,\ldots,N/2$ of the lattice of dimers (lattice constant $\mathbf{b}$). Equation (5) shows the two types of contributions which survive the limit $\lambda\to 0$, i.e., which are present in the noninteracting dimer limit: (i) one magnon excitations with energy $\omega=\pm J$ (related in strength by the detailed balance factor $e^{-\beta J}$); (ii) a contribution at $\omega=0$ which results from transitions (diagonal terms for S^{zz}) within the excited dimer triplet. It therefore carries a factor $e^{-\beta J}$ and will develop into a central peak for $\lambda\neq 0$. Since all

transition processes in this limit are localized, the only nontrivial wave vector dependence results from form factors related to the internal dimer structure: the intradimer distance $\mathbf{d}$ determines the "dimer structure factor" $(1-\cos \mathbf{q}\cdot\mathbf{d})$ and the corresponding factor $(1+\cos \mathbf{q}\cdot\mathbf{d})$ for the central contribution.

The result of Eq. (5) is independent of N since for independent dimers, $\lambda=0$, the correlation length vanishes and the exact result is obtained already for $N=1$. Increasing N only changes the number of wave vectors $\mathbf{q}$ and their positions. This guarantees the extensivity of the sum rule $\Sigma_{\mathbf{q}}\int d\omega S^{zz}(\mathbf{q},\omega)=N/4$.[20] The absolute intensity of the one-"magnon" peak at, e.g., $q=2\pi$ develops from $1/2$ at $T=0$ to $1/8$ at $T\to\infty$. We note that the various contributions to this intensity from states with a different number of excited dimers depend on N as can be identified easily from Eq. (5): The prefactor in Eq. (5),

$$\frac{1}{1+3e^{-\beta J}}=\frac{(1+3e^{-\beta J})^{N/2-1}}{(1+3e^{-\beta J})^{N/2}} \tag{6}$$

originates from the partition function in the denominator and the phase space factor resulting from excited dimers which do not participate in the transition in the numerator. The expansion of the numerator thus gives as a series the relative strength of the various contributions with energy J starting from a state with M excited dimers: The contribution of states with M excited dimers is proportional to $\binom{N/2}{M}(3e^{-\beta J})^M$. For $T\to\infty$ this reduces to $\binom{N/2}{M}3^M$, the degeneracy of states with M excited dimers. From this follows that the various contributions to the dynamic structure factor from states with M excited dimers have a well defined maximum (for $N\gg 1$) at $M=M_0=zN$ with $z=3/(e^{\beta J}+3)$. This means $M_0\approx 0.524N$ for $T=J$ and $M_0=0.75N$ for $T\to\infty$.

It should be noted that even for $T\to\infty$ the result of Eq. (5) is a quantum mechanical result reflecting the discrete energy spectrum of a $S=1/2$ dimer. It does not agree with the classical limit which is defined by the limit $\hbar\to 0$, i.e., for spins which are classical vectors or alternatively in the limit $S\to\infty$. From the latter approach follows that the frequency regime $0<\omega<2JS$ fills continuously with excitation strength in the classical limit. The result of Eq. (5) can clearly also be generalized to include an external magnetic field, a case which will be treated in a forthcoming paper.

Allowing for finite coupling λ several features appear: (i) the contributions at $\omega=0$ and $\omega=\pm J$ acquire a finite width owing to the dispersion of the excitations, (ii) additional contributions at $\omega\approx\pm pJ$ appear in increasing order in λ, (iii) the intradimer form factors get modified.[19] For small coupling $\lambda\ll 1$, two essential characteristics of the noninteracting limit survive qualitatively as shown for $N=20$, $\lambda=0.3$ in Fig. 1: The correlation length remains small and the density of states continues to show a well defined sequence of peaks with maxima at $E\approx pJ$ up to the upper bound of the spectrum and with widths of the order of λ independent of energy. Thus, the largest contributions to the transitions $\omega\approx J$ $(\omega\approx 2J)$, which start at energies $E\approx M_0\ J$ will be included for $N\geqslant 16$ $(N\geqslant 20)$ even for $T\to\infty$. We conclude that these system sizes will be sufficient to obtain reasonable results for the BAHC structure factor at moderate λ and all temperatures in its most interesting frequency regimes.

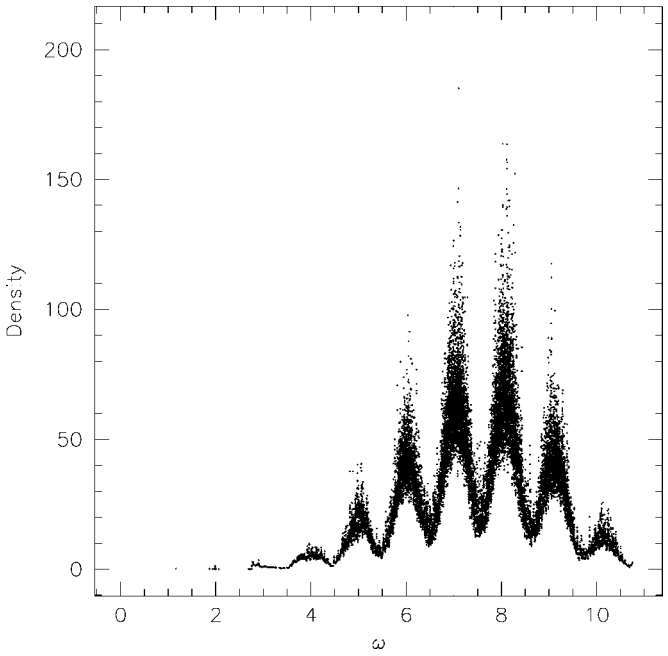

FIG. 1. Density of states for $N=20$, $\lambda=0.3$, $q=\pi$. Each point in the figure represents one multiplet.

For our numerical calculations we have used the Householder algorithm to obtain all eigenvalues and eigenvectors of the Hamiltonian in the subspace of constant S^z_{tot} and wave vector. Calculations were performed on workstations with Pentium IV processors at the ITP, Hannover University and on the JUMP supercomputer at NIC Jülich. Calculations for $N=16$ are comfortable to perform (matrix dimension is about 2000, required memory about 100 MB). A few calculations have been performed for $N=20$ for one value of λ and the wave vector and frequency regime where the bound triplet two magnon state is found; here memory (a few GB) and required CPU time are at the limit what can be reasonably managed at present.

III. RESULTS AND DISCUSSION

In this section we present our results for $S^{zz}(\mathbf{q},\omega)$. We cover the full range of temperatures (in units of J), $T=0.1\cdots T=4$ (the latter being representative for $T\to\infty$) and wave vectors q (in units of b^{-1}) from 0 to 2π. As standard values we use $N=16$ and $\lambda=0.3$. We find that the variation with λ for smaller values can be safely found from interpolating the results presented here. The number of spins strongly influences the level density and the discreteness of reciprocal space; however, the positions of levels which occur at identical wave vectors for different N (e.g., the one magnon state and the $S=1$ bound state below the two magnon band at wave vector π) do not change with N going from $N=12$ to $N=24$ (values for $N=24$ were obtained from Lanczos diagonalization). In this work we consider the simplest case $\mathbf{d}=\mathbf{b}/2$. Then d is the distance between all spins and it is sufficient to specify $q=|\mathbf{q}|$ in the following. $d=b/2$ implies

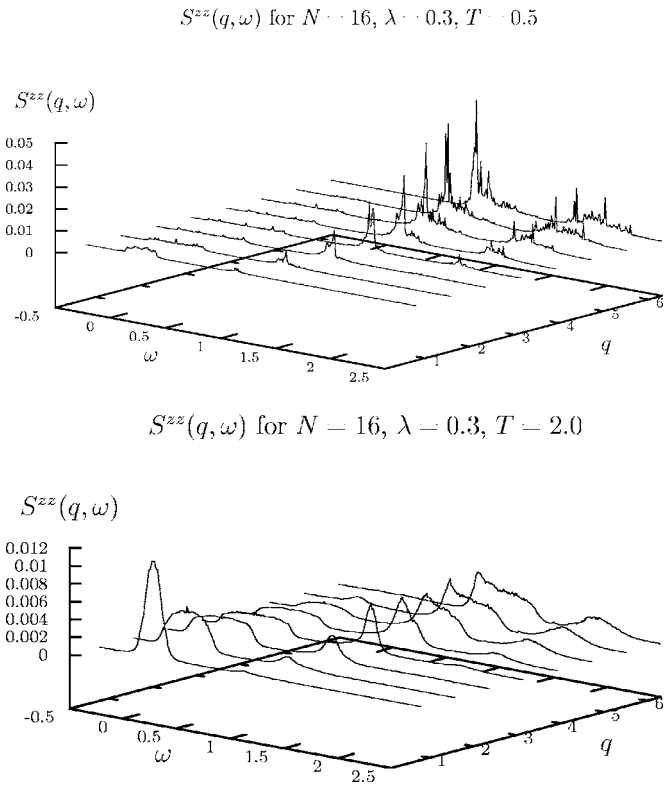

FIG. 2. Overall picture of the dynamic structure factor $S^{zz}(q,\omega)$ for $N=16$, $\lambda=0.3$, (a) $T=0.5$, (b) $T=2.0$. The intensity of the two magnon peaks is enlarged by the factor 20.

that the effects from the dimer form factors are particularly simple: in lowest orders the central contribution vanishes for $q=2\pi$ and the one magnon contribution for $q=0$. Temperatures and frequencies are given in units of J throughout this section. The complete variation of $S^{zz}(q,\omega)$ with wave vector and frequency for $N=16$ and $\lambda=0.3$ is shown in Fig. 2 for two temperatures, $T=0.5$ and $T=2$. The small contribution of the two-magnon excitations has been enlarged by a factor 20. The remaining figures display the details of the influence of temperature on the various interesting aspects of the spectra. The scale of $S^{zz}(q,\omega)$ is set by the value for the one magnon peak for noninteracting dimers at $T=0$ and $q=2\pi$, i.e., 1/2 in the units of Eq. (2). For all presentations the transitions strengths have been added up within frequency bins of mostly $\Delta\omega=0.01$ (0.002 in Fig. 6).

Figure 3 illustrates the evolution with temperature of the one-magnon peak for $N=16$ and $\lambda=0.3$. With increase in temperature, the peaks extend over a nearly constant range in frequency, although the decrease of the maximum of intensity formally implies an increase in the width at half maximum. For both $q=\pi$ and 2π the position of the maximum shifts to lower frequencies, but the peak develops a marked asymmetry with more intensity on the high frequency side. This effect is most pronounced for $q=2\pi$, the wave vector of the energy gap (and may not be the case at all for small values of q, see Fig. 2). Thus, the detailed description of the line shape provides an understanding for the puzzling observation that the gap energy seems to increase with temperature[6] (comparable to an analogous observation in the Haldane chain).[21] It would be interesting to compare the line shape to the result of the theoretical approach of Ref. 12. However, with $N=16$, a continuous line shape results only

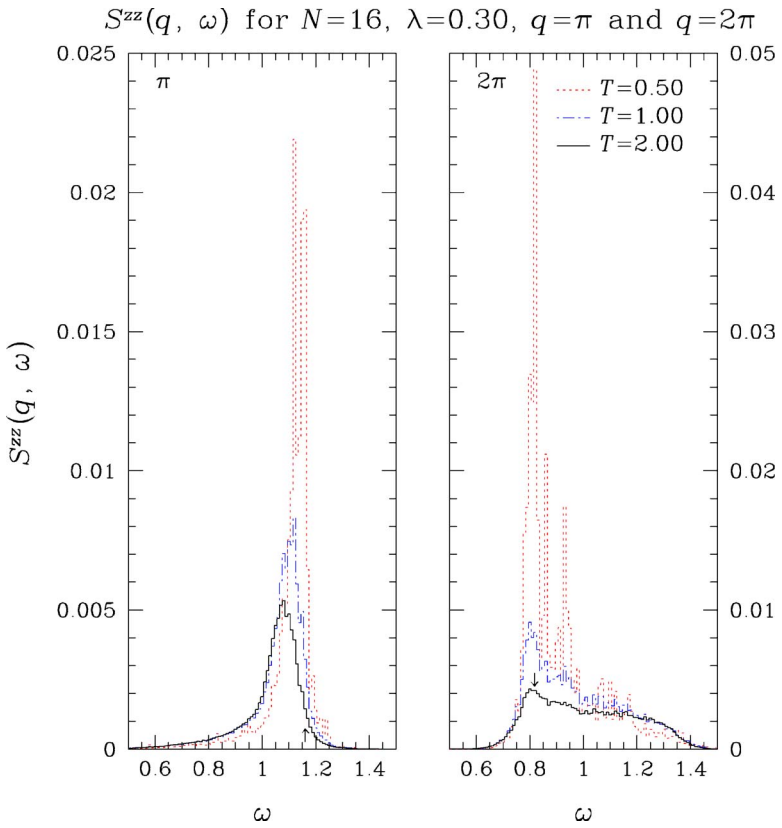

FIG. 3. (Color online) One-magnon peak for $N=16$, $\lambda=0.3$: (a) $q=\pi$ and (b) $q=2\pi$. Temperatures are $T=0.5$ (dotted lines), $T=1.0$ (dash-dotted lines), $T=2.0$ (full lines). The arrows indicate the frequencies of the one magnon transition at $T=0$.

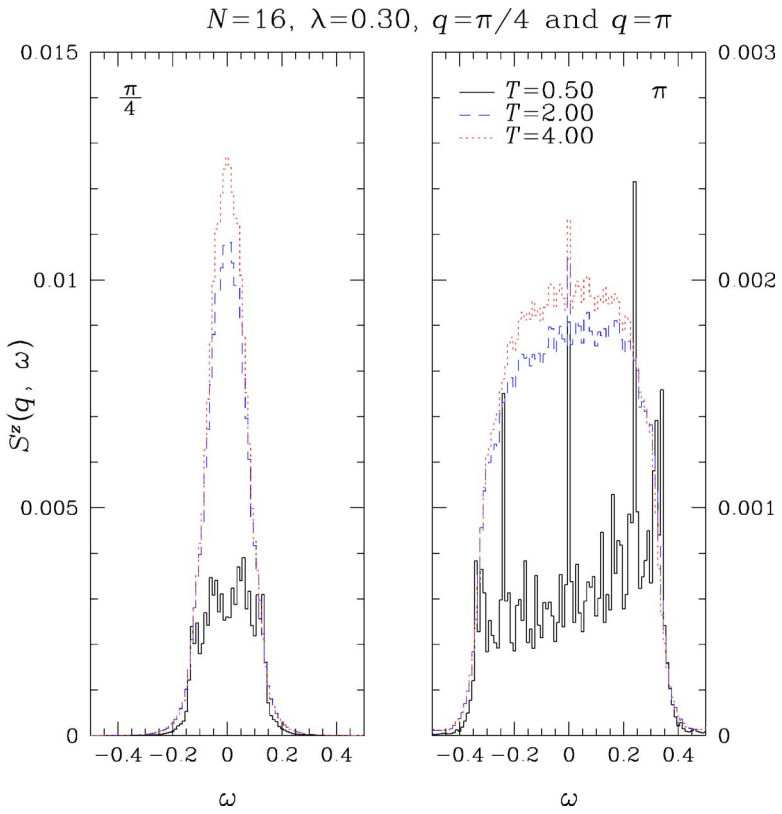

FIG. 4. (Color online) Central peak for $N=16$, $\lambda=0.3$: variation with temperature up to $T=4$ for (a) $q=\pi/4$ and (b) $q=\pi$.

for temperatures above the energy gap and is thus in the nonuniversal approach of the approach of Ref. 12. When we look at the microscopic origin of the peak broadening, we find that, e.g., at $T=1.0$ the basic transition from the ground state to the one magnon excitation at $q=\pi$ is responsible for 30% of the weight at that frequency and that for the neighboring frequencies transitions starting from the one-magnon band contribute about 10% of the total weight, whereas the by far largest part of the intensity originates from transitions starting at states with two or more excited dimers.

Figure 4 illustrates for $N=16$, $q=\pi/4$, and π the evolution of the central peak with temperature (for $\lambda=0.3$). At low T and $\lambda \ll 1$ the shape of the central peak is dominated by transitions inside the weakly interacting one magnon band with q-independent matrix elements. The physical process may be thought of as an external probe accelerating a thermally populated excitation and is thus similar to well known processes in soliton bearing 1D magnets.[22] As in these models, the limiting form of the structure factor is

$$S^{zz}_{(0)}(q,\omega) \propto e^{-\beta J} \frac{1}{\sqrt{1-\omega^2/\omega_m(q)^2}} \Theta[\omega_m^2(q)-\omega^2] \qquad (7)$$

with $\omega_m(q)=\lambda \sin(q/2)$ just from phase space effects (a small variation with temperature resulting from the dispersion has been neglected). Numerically we find that the cutoff of the central peak remains localized at $\omega \approx \omega_m(q)$ for all wave vectors and temperatures [apart from corrections of $\mathcal{O}(\lambda^2)$]. The line shape, however, cannot be expected to be reproduced since only a few discrete transitions in the one magnon band are available for $N=16$ and dominate the spectrum at the lowest temperatures. Nevertheless, for $q=\pi$, $T=0.5$ the inverted line shape of Eq. (7) starts to become visible even with this restriction. Between medium ($T=0.5$) and high ($T=4$) temperatures a crossover of the line shape from squarelike to Gaussian is observed for small wave vectors. In view of the experimental[23] and theoretical[24,25] discussion of spin diffusion in gapped 1D magnets we have also made a rough analysis of the linewidth variation with the wave vector. We find that the $T=4$ spectra fit surprisingly well to a Gaussian (but not to a Lorentzian) and the linewidth increases by a factor of about 5 upon doubling the wave vector from $q=\pi/4$ to $\pi/2$. This indicates that the crossover to spin-diffusion-like behavior governs the behavior of the DSF in the regime considered here. The decrease of the overall intensity with temperature due to the thermal occupation factor will be discussed below, see Fig. 7.

Figure 5 shows the two-magnon peak at $q=\pi$ (where the bound states are most clearly visible) and $q=2\pi$ for $N=16$, $\lambda=0.3$ in the temperature range $T=0.5\cdots 2$ (note the enhancement in frequency and intensity scales). For $q=\pi$ the low temperature spectra are entirely dominated by the $S=1$ bound state at $\omega \approx 1.938\ldots$, whereas the continuum (which at $T=0$ is smaller by a factor of λ^2 in intensity[18]) plays no significant role. The bound state remains clearly visible up to $T=1$ and then disappears in parallel with rapid decrease in the integrated intensity of the two-magnon peak for temperatures above $T=1$ (see also Fig. 7 below). This reflects the fact that dimers become independent of each other with increasing temperature such that the correlations between spins in two different dimers required for a finite two-magnon peak disappear. In Fig. 6 we present a comparison between results for $N=16$ and $N=20$ (available only for $q=\pi$ and the limited frequency range $1.84<\omega<2.02$). In going from N

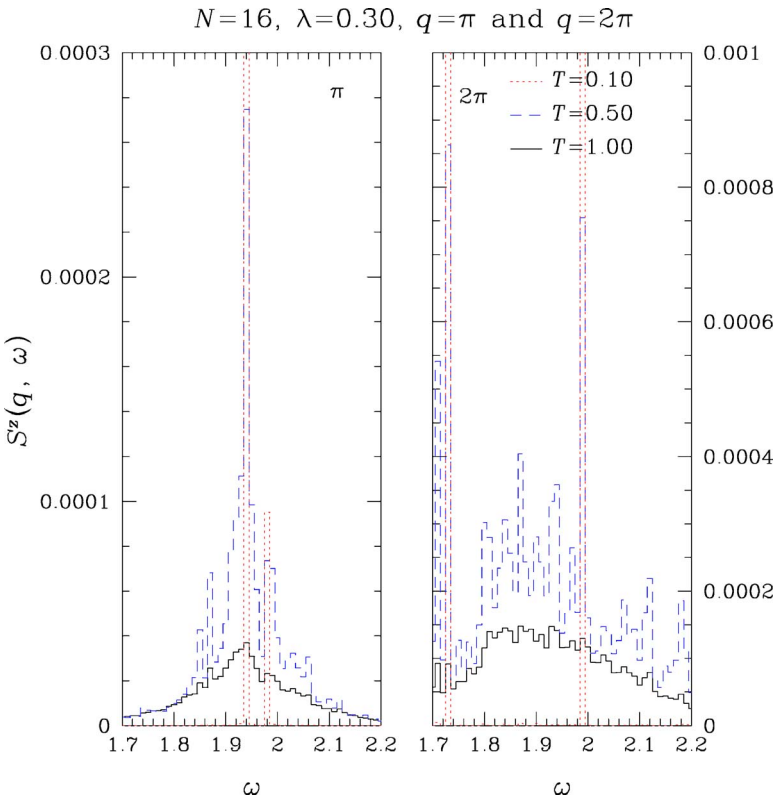

FIG. 5. (Color online) Two magnon peak for $N=16$, $\lambda=0.3$ and different temperatures (symbols as in Fig. 3): (a) $q=\pi$ (the $S=1$, $T=0.1$ bound state contribution is at 0.00318 outside the frame), (b) $q=2\pi$ (the two largest $T=0.1$ contributions are outside the frame at 0.0109 for $\omega \approx 1.73$ and at 0.009 61 for $\omega \approx 1.99$).

$=16$ to $N=20$ some improvement is obtained, the continuum becomes smoother and the bound state less dominant, but the main characteristics are unchanged. Thus, the increase in N is not really crucial. The spectra invoke the impression that at intermediate temperatures additional transitions (in particular the $S=0$ state at $\omega \approx 1.868$ which could be reached from a thermally excited $S=1$ state) become visible. This, however, is misleading as the comparison between the data

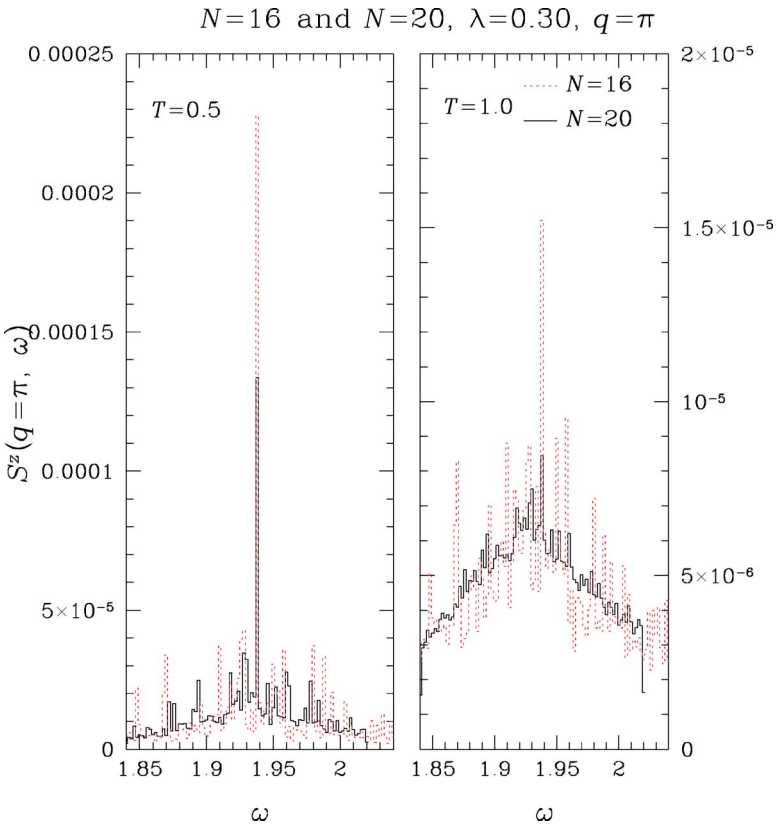

FIG. 6. (Color online) The two-magnon peak for $q=\pi$, $\lambda=0.3$ and $N=16$ and $N=20$ (for the frequency interval $1.84<\omega<2.02$) in comparison: (a) $T=0.5$ and (b) $T=1$. Here, narrow frequency bins, $\Delta\omega=0.002$, are used.

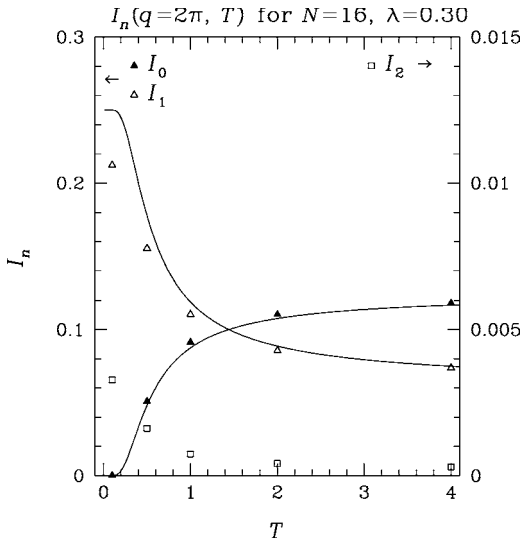

FIG. 7. Temperature dependence of the exclusive structure factors $I_n(q,T)$ for $N=16$, $\lambda=0.3$ and $q=\pi$. $n=0,1$ [left scale, lines give the result for $\lambda=0$ from Eq. (5)] and $n=2$ (right scale).

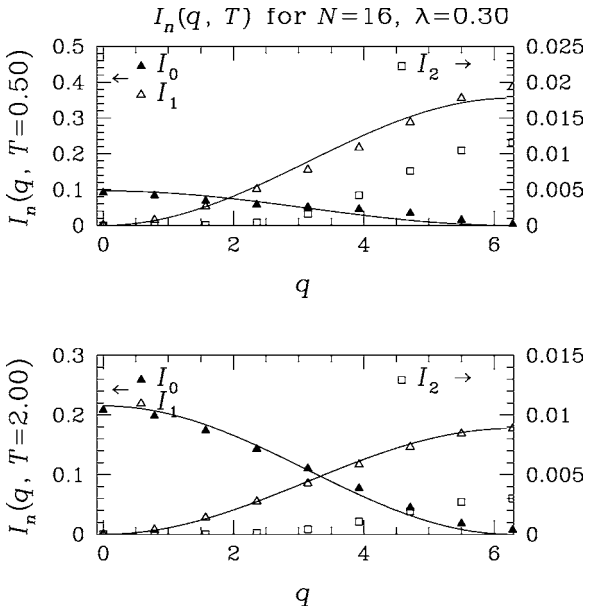

FIG. 8. Wave vector dependence of the exclusive structure factors $I_n(q,T)$ for (a) $T=0.5$ and $T=2.0$. Lines for $n=0,1$ give the result for $\lambda=0$ from Eq. (5). Units for I_2 (right scale) are enhanced by a factor of 20.

for $N=16$ and $N=20$ shows: A change in the number of spins leads to a different set of allowed wave vectors and thus, from the accompanying change in the initial and final energies, to trivially different excitation frequencies (although the energies at, e.g., $q=\pi$ are remarkably independent of N). For $q=2\pi$ there is no bound state; the two discrete transitions at $T\approx 0$ in Fig. 5(b) are the remainder of the continuum for the limited number of spins 16.

For a more global analysis we show in Fig. 7 the intensities $I_n(q=\pi,T)$ obtained from integrating $S^{zz}(q=\pi,\omega)$ over frequency intervals $(n-\frac{1}{2})<\omega<(n+\frac{1}{2})$. The results for $q=\pi$ are representative also for the other q values. These "exclusive structure factors" show most clearly the relevance of quantum fluctuations with increasing interdimer coupling λ at low temperatures. Quantum fluctuations are most important for the one-magnon peak I_1 at low temperatures. $I_1(q=\pi,T)$ comes close to its classical limit independent of λ at $T\approx 2$, whereas the temperature dependence of $I_0(q=\pi,T)$ follows closely the $\lambda=0$ result of Eq. (5) for all temperatures. The temperature variation of $I_2(q=\pi,T)$ shows clearly that an observation of the two-magnon peak requires low temperatures $T<1$. Transitions corresponding to exciting more than two dimers are extremely small in magnitude: A typical number is $I_3(q=2\pi,T=0.5)\approx 2\times 10^{-5}$. From further calculations of integrated intensities we conclude that the number of spins is not very important for the overall features: $N=12$ gives nearly undistinguishable results.

Figure 8 shows the influence of temperature and interdimer interaction on the dimer structure factor $(1-\cos qd)$ for the one-magnon intensity and the corresponding factor $(1+\cos qd)$ for the central peak. In the analysis of experiments this factor is usually considered as a prefactor independent of λ and ω, although it is clear already from the zero temperature analysis[19] that corrections are present in higher orders in λ. Figure 8 shows an overall agreement between the numerical results for $\lambda=0.3$ and those of the noninteracting limit although closer inspection reveals significant differences: The ratio $I_1(q=2\pi,T=0.5)/I_1(q=\pi,T=0.5)$, e.g., is about 2.5 for $\lambda=0.3$ compared to 2 for $\lambda=0$. Figure 8 also displays the wave vector dependence of the two-magnon peak which is absent in the noninteracting limit: The intensity of this peak depends strongly on wave vector and wave vectors $q>\pi$ are most favorable for an observation of these processes.

IV. CONCLUSIONS

We have calculated the dynamic structure factor of the bond alternating Heisenberg chain based on full exact diagonalization for chains with up to 20 spins 1/2. This allows us to obtain results at finite temperatures which cover the complete temperature range from $T\ll J$ to $T\gg J$. Our results are for dimerlike chains with sufficiently small interdimer exchange λJ. We find that the characteristics of the noninteracting dimer limit [where the full temperature dependent structure factor, Eq. (5), is easily available analytically] describe much of the interacting BAHC. This is demonstrated here for $\lambda=0.3$ (but is essentially true up to typically $\lambda\approx 0.5$) and applies in particular to the existence of the central (zero frequency) peak and to the temperature and wave vector dependence of the integrated intensities (exclusive structure factors) for the central and the one-magnon peak. This large range of validity of the dimer picture is in agreement with the observation[26] that the dimer picture gives a good account of excitation strengths up to and including the isotropic limit of the HAF at zero temperature.

Experimental and theoretical interest in the dynamics of the BAHC results from the possibility that this theoretical model and its realizations in a number of materials might serve as simple model systems to discuss the interplay be-

tween temperature and quantum fluctuations. Our results reveal that this interplay becomes apparent in a number of points which are accessible to experimental, in particular neutron scattering, observations:

(i) The shape of the central peak which is a prominent feature of the BAHC, displays the crossover with temperature from the noninteracting particlelike behavior at low temperatures to the diffusive behavior at high temperatures.

(ii) The one-magnon peak develops an asymmetric linewidth (with appreciable strength on the high frequency side) with temperature. This is particularly evident for wavevector $q=2\pi$ at temperatures $T\geqslant 1$ and appears to describe in more detail the upward shift in gap energy with temperature noted in approximate theoretical approaches.

(iii) The two magnon peak (around $q=\pi$) is dominated by the bound triplet state on top of a small continuum which is smooth at all temperatures and wavevectors.

The results as presented here are restricted to the basic situation of equidistant spins and isotropy implying the absence of an external magnetic field. In subsequent work we will extend the calculations to cover the finite temperature dynamics in an external magnetic field and also to describe real materials such as $Cu(NO_3)_2$ and $(VO)_2P_2O_7$. We will also investigate in more detail the regime $\lambda>0.5$, approaching the isotropic (Heisenberg) limit in order to study stronger deviations from the dimerlike situation.

ACKNOWLEDGMENTS

We wish to thank M. Enderle, A. K. Kolezhuk, S. Notbohm, and D. A. Tennant for stimulating discussions. We gratefully acknowledge that computational facilities for the numerical calculations were generously provided by the John von Neumann-Institut for Computing at Jülich Research Center.

[1] D. A. Tennant, C. Broholm, D. H. Reich, S. E. Nagler, G. E. Granroth, T. Barnes, K. Damle, G. Xu, Y. Chen, and B. C. Sales, Phys. Rev. B **67**, 054414 (2003).

[2] M. Jaime, V. F. Correa, N. Harrison, C. D. Batista, N. Kawashima, Y. Kazuma, G. A. Jorge, R. Stein, I. Heinmaa, S. A. Zvyagin, Y. Sasago, and K. Uchinokura, Phys. Rev. Lett. **93**, 087203 (2004); S. E. Sebastian, P. A. Sharma, M. Jaime, N. Harrison, V. Correa, L. Balicas, N. Kawashima, C. D. Batista, and I. R. Fisher, Phys. Rev. B **72**, 100404(R) (2005).

[3] T. Kato, K. Takatsu, H. Tanaka, W. Shiramura, M. Mori, K. Nakajima, and K. Kakurai, J. Phys. Soc. Jpn. **67**, 752 (1998); K. Takatsu, W. Shiramura, and H. Tanaka, *ibid.* **66**, 1611 (1997).

[4] N. Cavadini, Ch. Rüegg, W. Henggler, A. Furrer, H.-U. Güdel, K. Krämer, and H. Mutka, Eur. Phys. J. B **18**, 565 (2000).

[5] S. Notbohm, D. A. Tennant, B. Lake, P. C. Canfield, J. Fielden, P. Koeglerer, H.-J. Mikeska, and M. T. F. Telling (unpublished).

[6] Ch. Rüegg, B. Normand, M. Matsumoto, Ch. Niedermayer, A. Furrer, K. W. Krämer, H.-U. Güdel, Ph. Bourges, Y. Sidis, and H. Mutka, Phys. Rev. Lett. **95**, 267201 (2005).

[7] K. Fabricius, U. Löw, and K. H. Mütter, Phys. Rev. B **51**, 8270 (1995); K. Fabricius, U. Löw and J. Stolze, *ibid.* **55**, 5833 (1997).

[8] K. Fabricius and U. Löw, Phys. Rev. B **57**, 13371 (1998).

[9] A. Bühler, U. Löw, and G. S. Uhrig, Phys. Rev. B **64**, 024428 (2001).

[10] K. P. Schmidt, H. Monien, and G. S. Uhrig, Phys. Rev. B **67**, 184413 (2003).

[11] M. Troyer, H. Tsunetsugu, and D. Würtz, Phys. Rev. B **50**, 13515 (1994).

[12] K. Damle and S. Sachdev, Phys. Rev. B **57**, 8307 (1998).

[13] S. Brehmer, H. J. Mikeska, and U. Neugebauer, J. Phys.: Condens. Matter **8**, 7161 (1996).

[14] G. Squires, *Thermal Neutron Scattering* (Cambridge University Press, Cambridge, 1978).

[15] G. S. Uhrig and H. J. Schulz, Phys. Rev. B **54**, R9624 (1996).

[16] T. Barnes, J. Riera, and D. A. Tennant, Phys. Rev. B **59**, 11384 (1999).

[17] S. Trebst, H. Monien, C. J. Hamer, Z. Weihong, and R. R. P. Singh, Phys. Rev. Lett. **85**, 4373 (2000).

[18] C. J. Hamer, W. Zheng, and R. R. P. Singh, Phys. Rev. B **68**, 214408 (2003).

[19] M. Müller, H. J. Mikeska, and N. Cavadini, J. Phys.: Condens. Matter **15**, 8513 (2003).

[20] We note that in our definition of reciprocal space the summation extends over the large Brillouin zone $(0<q<4\pi/b)$, corresponding to the basic distance $d=b/2$ between spins.

[21] Th. Jolicoeur and O. Golinelli, Phys. Rev. B **50**, 9265 (1994); J. P. Renard, M. Verdaguer, L. P. Regnault, W. A. C. Erkelenz, J. Rossat-Mignot, and W. G. Stirling, Europhys. Lett. **3**, 945 (1987); J. P. Renard, M. Verdaguer, L. P. Regnault, W. A. C. Erkelenz, J. Rossat-Mignot, J. Ribas, W. G. Stirling, and C. Vettier, J. Appl. Phys. **63**, 3538 (1988).

[22] J. Villain, Physica B & C **79B**, 1 (1975).

[23] M. Takigawa, T. Asano, Y. Ajiro, M. Mekata, and Y. J. Uemura, Phys. Rev. Lett. **76**, 2173 (1996).

[24] J. Karadamoglou and X. Zotos, Phys. Rev. Lett. **93**, 177203 (2004).

[25] K. Damle and S. Sachdev, Phys. Rev. Lett. **95**, 187201 (2005).

[26] K. P. Schmidt and G. S. Uhrig, Phys. Rev. Lett. **90**, 227204 (2003).